◆ Human Brain Mapping 37:3080–3102 (2016) ◆

Axon Density and Axon Orientation Dispersion in Children Born Preterm

Claire E. Kelly,[1]* Deanne K. Thompson,[1,2,3] Jian Chen,[1,4] Alexander Leemans,[5] Christopher L. Adamson,[1] Terrie E. Inder,[6] Jeanie L.Y. Cheong,[1,7,8] Lex W. Doyle,[1,3,7,8] and Peter J. Anderson[1,3]

[1]*Murdoch Childrens Research Institute, Melbourne, Australia*
[2]*Florey Institute of Neuroscience and Mental Health, Melbourne, Australia*
[3]*Department of Paediatrics, University of Melbourne, Melbourne, Australia*
[4]*Department of Medicine, Monash Medical Centre, Monash University, Melbourne, Australia*
[5]*Image Sciences Institute, University Medical Center Utrecht, Utrecht, The Netherlands*
[6]*Brigham and Women's Hospital, Boston, Massachusetts*
[7]*Royal Women's Hospital, Melbourne, Australia*
[8]*Department of Obstetrics and Gynaecology, University of Melbourne, Melbourne, Australia*

Abstract: *Background:* Very preterm birth (VPT, <32 weeks' gestation) is associated with altered white matter fractional anisotropy (FA), the biological basis of which is uncertain but may relate to changes in axon density and/or dispersion, which can be measured using Neurite Orientation Dispersion and Density Imaging (NODDI). This study aimed to compare whole brain white matter FA, axon dispersion, and axon density between VPT children and controls (born ≥37 weeks' gestation), and to investigate associations with perinatal factors and neurodevelopmental outcomes. *Methods:* FA, neurite dispersion, and neurite density were estimated from multishell diffusion magnetic resonance images for 145 VPT and 33 control 7-year-olds. Diffusion values were compared between groups and correlated with perinatal factors (gestational age, birthweight, and neonatal brain abnormalities) and neurodevelopmental outcomes (IQ, motor, academic, and behavioral outcomes) using Tract-Based Spatial Statistics. *Results:* Compared with controls, VPT children had lower FA and higher axon dispersion within many major white matter fiber tracts. Neonatal brain abnormalities predicted lower FA and higher axon dispersion in many major tracts in VPT children. Lower FA, higher axon dispersion, and lower axon density in various tracts correlated with poorer neurodevelopmental outcomes in VPT children. *Conclusions:* FA and NODDI measures distinguished VPT children from controls and were asso-

Additional Supporting Information may be found in the online version of this article.

Contract grant sponsor: National Institutes of Health (NIH); Contract grant numbers: R01 HD05709801, P30 HD062171, and UL1 TR000448 to T.E.I.; Contract grant sponsor: The National Health and Medical Research Council (NHMRC) of Australia; Contract grant number: Project Grant No. 237117 to T.E.I. and L.W.D.; Project Grant No. 491209 to P.J.A., T.E.I. and L.W.D.; Contract grant sponsor: Centre of Research Excellence; Contract grant number: No. 1060733 to L.W.D., P.J.A, J.L.Y.C. and D.K.T.; Contract grant sponsor: Senior Research Fellowship; Contract grant number: No. 1081288 to P.J.A.; Contract grant sponsor: Career Development Fellowship; Contract grant number: No. 1085754 to D.K.T.; Contract grant sponsor: Early Career Fellowship; Contract grant numbers: No. 1012236 to D.K.T. and 1053787 to J.L.Y.C; Contract grant sponsor: the United Cerebral Palsy Foundation, The United States to T.E.I.; Contract grant sponsors: The Victorian Government's Operational Infrastructure Support Program, the Royal Children's Hospital Foundation, and the Netherlands Organisation for Scientific Research (NWO); Contract grant number: VIDI Grant 639.072.411 to A.L.

*Correspondence to: Claire E. Kelly; Victorian Infant Brain Study (VIBeS), Murdoch Childrens Research Institute, The Royal Children's Hospital, Flemington Road, Parkville, Victoria, 3052, Australia. E-mail: claire.kelly@mcri.edu.au

Received for publication 7 March 2016; Accepted 12 April 2016.

DOI: 10.1002/hbm.23227

Published online 2 May 2016 in Wiley Online Library (wileyonlinelibrary.com).

ciated with neonatal brain abnormalities and neurodevelopmental outcomes. This study provides a more detailed and biologically meaningful interpretation of white matter microstructure changes associated with prematurity. *Hum Brain Mapp 37:3080–3102, 2016.*

Key words: magnetic resonance imaging; diffusion-weighted imaging; diffusion tensor imaging; NODDI; white matter; neurodevelopment; preterm birth

INTRODUCTION

Very preterm (VPT) birth (<32 weeks' gestation) is a significant public health concern. VPT birth is a leading cause of neonatal mortality and morbidity worldwide, and many VPT survivors develop long-term delays in multiple neurodevelopmental domains including cognition, movement, academic performance, and behavior [Anderson, 2014; Arpino et al., 2010; Hutchinson et al., 2013; Spittle and Orton, 2014; Sutton and Darmstadt, 2013]. Studying brain injury and development in VPT children is of high priority, as knowledge of the underlying neurobiological changes is necessary for: (1) establishing biomarkers for identifying at-risk VPT children who warrant close surveillance and early intervention; (2) assessing the efficacy of interventions to treat or prevent neurodevelopmental disabilities; (3) reducing the overall burden of VPT birth on infant health and development and health-care resources [Counsell et al., 2014; Duerden et al., 2013].

Brain injury in VPT infants primarily targets premyelinating oligodendrocytes within the developing cerebral white matter [Volpe et al., 2011], but can also involve the thalamus, basal ganglia, cerebral cortex, brainstem, and cerebellum in a constellation referred to as the encephalopathy of prematurity [Volpe, 2009]. Diffusion magnetic resonance imaging (MRI) analysis techniques such as diffusion tensor imaging (DTI) provide a method for probing brain tissue microstructure non-invasively [Jones et al., 2013]. DTI generates whole brain, voxelwise quantitative parameters such as fractional anisotropy (FA), which measures the degree to which diffusion is directionally restricted [Jones et al., 2013]. FA is generally high within cerebral white matter, where diffusion is restricted along the length of fibers due to the presence of barriers such as axon membranes and myelin. Previous studies of FA values within the white matter of preterm groups have generally found that FA is lower in preterm groups compared with control groups born at term (≥37 weeks' gestation) in widely distributed fiber tracts in infancy and through to early adulthood, as recently reviewed in detail [Ment et al., 2009; Pandit et al., 2013]. In line with this, previous studies by our group and others have also found that lower FA in preterm children is predicted by perinatal medical factors relating to preterm birth [particularly neonatal brain abnormalities, lower gestational age (GA) at birth and lower birthweight], and is associated with neurodevelopmental delays [Kelly et al., 2015a, 2015b, 2014; Ment et al., 2009; Pandit et al., 2013; Pannek et al., 2014; Thompson et al., 2014b,].

While FA has proven to be sensitive to changes in brain white matter microstructure, interpretation of FA changes on the cellular scale is ambiguous. This is because the degree to which diffusion is directionally restricted within white matter depends on numerous microstructural properties, including the axon diameter, axon density, membrane permeability, myelination, axon orientation distributions (e.g., whether there are bending, fanning, or crossing axons), and contributions from non-white matter tissue types such as cerebrospinal fluid (CSF) [Jones et al., 2013]. Therefore changes in FA cannot be attributed directly to changes in any single aspect of white matter microstructure [Jones et al., 2013; Vos et al., 2011, 2012]. Given this, there has been recent focus on developing diffusion MRI analysis techniques that can relate the diffusion signal more directly and specifically to underlying cellular microstructural properties. One such technique, Neurite Orientation Dispersion and Density Imaging (NODDI), enables the analysis of two key factors that may contribute to changes in FA—the orientation dispersion and the density of neurites (axons or dendrites in the white matter or gray matter, respectively) [Zhang et al., 2012]. Lower FA values within white matter are expected to be caused by increases in the dispersion of axons, or decreases in the density of axons, or both (among other factors) [Zhang et al., 2012]. Indeed, from preliminary work in the adult brain, FA within white matter shows a strong negative correlation with axon dispersion and a slightly weaker positive correlation with axon density [Zhang et al., 2012]. Therefore, lower white matter FA values associated with VPT birth, perinatal complications and neurodevelopmental delays could be due at least in part to increases in axon dispersion and/or decreases in axon density, but until now this hypothesis has not been tested.

The overall aim of this study was to apply NODDI to brain MRI scans of VPT children, in order to assess the contributions of axon dispersion and axon density to the white matter microstructure changes seen in this vulnerable population. Specifically, the first aim was to compare whole brain white matter FA, axon dispersion and axon density between VPT children and controls. We hypothesized that VPT children would have lower FA in widely distributed white matter fiber tracts compared with controls, which would be accompanied by increased axon dispersion and decreased axon density. The second aim was

to identify potential perinatal predictors of whole brain white matter FA, axon dispersion and axon density in VPT children. The hypothesis was that neonatal brain abnormalities, lower GA at birth and lower birthweight would predict lower FA in widespread fiber tracts in VPT children, along with increased axon dispersion and decreased axon density. The third aim was to investigate whether whole brain white matter FA, axon dispersion, and axon density are associated with neurodevelopmental outcomes in VPT children. The hypothesis was that lower FA in widespread fiber tracts in VPT children would be associated with poorer neurodevelopmental outcomes (worse IQ, motor function and academic performance, and more behavioral and emotional problems), which would be related to increases in axon dispersion and decreases in axon density.

MATERIALS AND METHODS

Participants

224 VPT infants (born <30 weeks' GA and/or <1250 g birthweight) and 46 controls (born ≥37 weeks' GA) were recruited during the neonatal period, between July 2001 and December 2003, from the Royal Women's Hospital, Melbourne into a prospective longitudinal study, as previously described [Thompson et al., 2007]. Infants with genetic or congenital abnormalities likely to affect development were excluded. At 7 years of age, participants were invited to attend a follow-up involving MRI and neurodevelopmental assessments. Of the originally recruited participants, 198 (88% of those recruited) VPT and 43 (93% of those recruited) control participants attended the 7-year follow-up, of whom 159 VPT and 36 control participants underwent MRI following mock MRI training. Diffusion MRI data could be analyzed in the current study for 145 VPT children (65% of the original sample) and 33 controls (72% of the original sample); that is, 14 VPT participants and 3 controls who underwent MRI were not included in the current study because: (1) they did not have diffusion images acquired ($n = 2$); (2) they had only one diffusion shell (either the $b = 1200$ s/mm^2 shell or the $b = 3000$ s/mm^2 shell but not both) ($n = 11$); (3) their diffusion images were incomplete due to excessive participant motion ($n = 1$); or (4) they were scanned with an incorrect diffusion sequence ($n = 3$).

Compared with VPT non-participants (who were originally recruited but did not contribute data to the current study; $n = 79$), VPT participants (who contributed data to the current study; $n = 145$) had slightly lower neonatal brain abnormality scores [median (25th–75th percentile)= 5 (4–9) vs. 5 (3–7.5) for VPT non-participants and VPT participants, respectively]. Fewer VPT participants were exposed to postnatal corticosteroids compared with VPT non-participants (6% vs. 16%). Other perinatal characteristics [GA at birth, birth weight, birth weight standard deviation (SD) score, and proportions of males, cystic periventricular leukomalacia (PVL), intraventricular hemorrhage (IVH) grade 3/4, postnatal infection, antenatal corticosteroid exposure, bronchopulmonary dysplasia, and small for GA births] were similar between VPT participants and VPT non-participants. Perinatal characteristics were also similar between control participants ($n = 33$) and control non-participants ($n = 13$).

Ethical approval for the study was obtained from the Human Research Ethics Committees of The Royal Women's Hospital and The Royal Children's Hospital, Melbourne. Written informed consent for the study was obtained from parents.

Perinatal Data

Perinatal data were collected by chart review during the primary hospitalization. Clinically relevant perinatal factors of interest in the current study were GA at birth and birthweight SD score, which was computed relative to the British Growth Reference [Cole et al., 1998]. Additionally, neonatal brain abnormality was scored qualitatively from T_2-weighted structural images acquired at term-equivalent age (37–44 weeks' GA), and a total neonatal brain abnormality score was calculated, as previously described and validated [Kidokoro et al., 2013].

MRI Acquisition

At 7 years of age, participants underwent MRI in a 3T scanner (Siemens Magnetom Trio, Tim system). Diffusion-weighted images were acquired based on twice-refocused echo planar imaging sequences. Two diffusion shells were acquired: (1) b-values ranging up to 1,200 s/mm^2, 25 non-collinear gradient directions in total, one $b = 0$ s/mm^2 volume; sequence parameters were: repetition time (TR) = 12,000 ms, echo time (TE) = 96 ms, field of view (FOV) = 250 × 250 mm, matrix size = 144 × 144, voxel size = 1.7 mm^3; 2) b-values of 3,000 s/mm^2, 45 non-collinear gradient directions in total, six $b = 0$ s/mm^2 volumes; sequence parameters were: TR = 7,400 ms, TE = 106 ms, FOV = 240 × 240 mm, matrix size = 104 × 104, voxel size = 2.3 mm^3.

Pre-Processing and Model Fitting

DTI fitting was performed using the $b = 1{,}200$ s/mm^2 shell. Prior to fitting, this shell was corrected for motion and eddy current induced distortions using the Functional MRI of the Brain Software Library (FSL) version 5.0.8, and the b-vectors were reoriented following motion correction [Leemans and Jones, 2009]. The weighted linear least squares tensor fitting method was employed using FSL [Veraart et al., 2013], from which FA images were generated.

NODDI fitting was performed using the $b = 1{,}200$ s/mm^2 and $b = 3{,}000$ s/mm^2 shells. The NODDI model

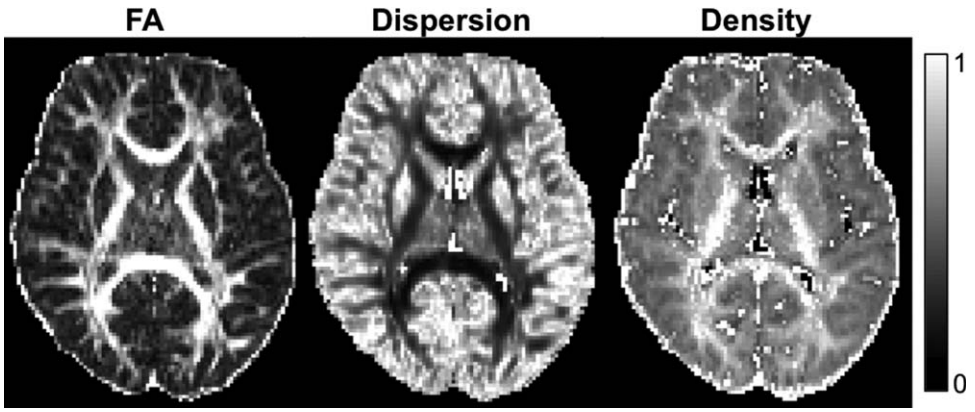

Figure 1.
Examples of images produced by NODDI (neurite dispersion and neurite density), shown for comparison against a fractional anisotropy (FA) image.

separates the diffusion signal into three compartments: intracellular, extracellular, and CSF [Zhang et al., 2012]. The intracellular compartment is modeled as sticks (cylinders of zero radius), to reflect diffusion that is restricted by neurites (any projection from a neuronal cell body; axons or dendrites in the brain white matter or gray matter, respectively). The orientation distribution of the sticks in the intracellular compartment is modeled by a Watson distribution, and provides an index of the orientation dispersion of neurites. In the brain white matter, this neurite orientation dispersion index (range 0–1) characterizes the spectrum of axon orientation patterns, from coherently aligned axons with low dispersion to bending, fanning or crossing axons with high dispersion. The volume fraction of the intracellular compartment (range 0–1) provides an index of the density of axons in the white matter (Fig. 1).

Prior to NODDI model fitting, the $b = 3{,}000$ s/mm^2 shell was registered to the $b = 1{,}200$ s/mm^2 shell using the Linear Image Registration Tool (FLIRT) within FSL [Jenkinson et al., 2002]. The aligned $b = 3{,}000$ s/mm^2 shell was then merged with the $b = 1{,}200$ s/mm^2 shell, and motion and eddy current distortion correction was performed on the combined volumes using FSL. Additionally, to account for the different TE and TR between the two shells, each shell was normalized by the $b = 0$ s/mm^2 image for that shell as per the developers' recommendation, which involved dividing every voxel in each shell by the average $b = 0$ s/mm^2 measurement for that shell [Owen et al., 2014]. NODDI model fitting and parameter estimation were performed using the NODDI Matlab toolbox version 0.9 [Zhang et al., 2012], generating neurite dispersion and density images.

For 42 (29%) of the VPT participants and 9 (27%) of the control participants, non-optimal $b = 3{,}000$ s/mm^2 images were acquired with diffusion gradient directions that were distributed non-uniformly on the sphere. NODDI images generated from the $b = 3{,}000$ s/mm^2 data acquired with versus without non-uniform gradient directions appeared qualitatively similar. However, statistical analyses were repeated for a subset excluding those participants whose $b = 3{,}000$ s/mm^2 images were acquired with non-uniform directions to ensure the non-uniform directions did not influence the results. The statistical analyses did not need to be repeated for the FA images, as the FA images were generated from the $b = 1{,}200$ s/mm^2 data, which were acquired with uniform gradient directions.

Tract-Based Spatial Statistics

FA, neurite dispersion, and neurite density images were analyzed using Tract-Based Spatial Statistics (TBSS), part of FSL [Smith et al., 2006]. Steps performed included: (1) aligning each participant's FA image to every other participant's FA image using FSL's nonlinear registration tool (FNIRT) [Andersson et al., 2007a,b]; (2) identifying the single most representative FA image as the study-specific target FA image; (3) aligning the study-specific target image to MNI152 1 × 1 × 1 mm standard space; (4) bringing all FA images to MNI152 1 × 1 × 1 mm standard space by combining their registration to the target with the registration from the target to MNI152 1 × 1 × 1 mm standard space; (5) generating a mean FA image and mean FA skeleton with an FA threshold of 0.2 (the generally recommended FA threshold, which based on visual inspection was shown to retain the major white matter tracts whilst minimizing inclusion of non-white matter voxels and voxels at the outermost edges of the images that have high inter-subject variability); (6) projecting each aligned FA image onto the mean FA skeleton; (7) applying the original nonlinear registrations to the neurite dispersion and density images and projecting the aligned neurite dispersion and density images onto the mean FA skeleton.

Neurodevelopmental Assessment

Neurodevelopmental assessments were conducted at 7 years corrected age. Neurodevelopmental domains assessed

and of interest in the current study included IQ estimated using the 4-subtest Wechsler Abbreviated Scale of Intelligence (WASI) [Wechsler, 1999], motor function using the Movement Assessment Battery for Children-2nd Edition (Movement ABC-2) [Henderson et al., 2007], academic performance (math computation and reading) using the Wide Range Achievement Test-4th Edition (WRAT-4) [Wilkinson and Robertson, 2006], and behavioral and emotional problems using the Strengths and Difficulties Questionnaire (SDQ) [Goodman, 1997]. For the WASI, Movement ABC-2 and WRAT-4 assessments, age standardized scores were used with higher scores indicating better performance. For the SDQ, the total raw score was used with higher scores indicating more behavioral/emotional problems.

Statistical Analysis

Voxelwise statistical analyses of the skeletonized FA, neurite dispersion, and neurite density images were performed using Randomise (version 2.9), FSL's tool for nonparametric permutation based testing of neuroimaging data [Nichols and Holmes, 2002; Winkler et al., 2014]. Firstly, groupwise (VPT vs. controls) comparisons of FA, neurite dispersion and neurite density across the skeleton were conducted, using two-sample unpaired *t*-test designs. Interactions between group (VPT vs. controls) and sex of the child (male vs. female) were also tested for. Secondly, correlations between perinatal factors and FA, neurite dispersion and neurite density across the skeleton in VPT children were investigated separately for each perinatal factor. When correlations were identified, the remaining perinatal variables were added into the model in order to adjust for their effect and identify independent perinatal predictors. Thirdly, correlations between FA, neurite dispersion and neurite density in VPT children and neurodevelopmental outcomes were investigated separately for each measure. In all statistical tests, 5,000 permutations were performed and age at MRI (corrected for prematurity) was included as a covariate of no interest to adjust for its potential effect. All results are reported at $P < 0.05$ after threshold-free cluster enhancement (TFCE) [Smith and Nichols, 2009] and family-wise error rate correction. Regions of statistical significance ($P < 0.05$, after TFCE and family-wise error rate correction) were localized to white matter tracts using the John Hopkins University (JHU) white-matter tractography atlas and the JHU ICBM-DTI-81 white-matter labels atlas [Hua et al., 2008].

RESULTS

Participants

Characteristics of the 145 VPT participants and 33 control participants are shown in Table I. As expected, the VPT group differed from the control group in relation to several perinatal characteristics, including having higher rates of postnatal and antenatal corticosteroid exposure, bronchopulmonary dysplasia, postnatal infection, small for GA births and patent ductus arteriosus, lower rates of singleton births, and longer stays at hospital. Median neonatal brain abnormality score was higher in the VPT group compared with controls, as expected. There were higher rates of major neonatal brain injury [cystic PVL and/or IVH grade 3/4] in the VPT group compared with controls, although overall relatively few VPT children had major neonatal brain injury. For characteristics at the 7-year assessment, the VPT group performed poorer than controls in the measures of IQ, motor ability, math computation, reading, and behavioral/emotional problems.

VPT Children Compared with Controls

There was a cluster of voxels that had lower FA in VPT children compared with controls, which was located within parts of the white matter tracts listed in Table II and shown in Figure 2A. There were no voxels where FA was *higher* in VPT children compared with controls. In addition, there were many voxels that had higher axon dispersion in VPT children compared with controls, located within the same tracts that had lower FA in VPT children compared with controls, as well as several other tracts (Table II, Fig. 2B). There were no voxels where axon dispersion was *lower* in VPT children compared with controls. When the participants whose $b = 3{,}000$ s/mm^2 diffusion images were acquired with non-uniform gradient directions were excluded from the analyses, there remained many voxels where axon dispersion was higher in VPT children compared with controls, although these voxels were slightly less widespread across the white matter and the significance of the differences was reduced (Supporting Information Table I; Supporting Information Fig. 1A). There were no voxels where axon density differed between VPT children and controls, and there were no interactions between birth group and sex of the child (i.e., the VPT vs. control group differences were similar for the sexes). FA, axon dispersion and axon density values, from the cluster of voxels that had significantly lower FA in the VPT group compared with controls, are plotted in Figure 3 and summarized in Table III. As Supporting Information to aid the reader in understanding the FA and NODDI values, we have also provided axial, radial and mean diffusivity values within the cluster that had lower FA in the VPT group (Supporting Information Fig. 2; Supporting Information Table II). This supplementary material shows that within the cluster that had lower FA in the VPT group, axial diffusivity was lower and radial and mean diffusivities were higher.

To investigate the effect of prematurity independent of children who had major brain injury in the neonatal period, we repeated the VPT versus controls analyses excluding the 10 VPT children who had IVH grade 3/4 and/or cystic PVL. The results were similar to the original analysis including all children, in that there remained lower FA and higher axon dispersion in VPT children

TABLE I. Participant characteristics

	VPT, $n = 145$	Controls, $n = 33$
Gestational age at birth (weeks), mean (SD)	27.5 (1.9)	38.9 (1.3)
Birthweight (g), mean (SD)	974 (226)	3,244 (501)
Birthweight SD score, mean (SD)	−0.5 (0.9)	0.0 (0.9)
Males, *n* (%)	71 (49)	16 (48)
Neonatal brain abnormality score, median (25th–75th percentile)	5 (3–7.5)[a]	1 (1–2.5)
Intraventricular hemorrhage grade 3/4, *n* (%)	5 (3)	0 (0)
Cystic periventricular leukomalacia, *n* (%)	5 (3)	0 (0)
Postnatal corticosteroids, *n* (%)	8 (6)[b]	0 (0)
Antenatal corticosteroids, *n* (%)	127 (88)[b]	0 (0)
Bronchopulmonary dysplasia, *n* (%)	45 (31)	0 (0)
Postnatal infection,[c] *n* (%)	46 (32)	1 (3)
Small for gestational age, *n* (%)	12 (8)	1 (3)
Singleton, *n* (%)	74 (51)	31 (94)
Patent ductus arteriosus, *n* (%)	68 (47)	0 (0)
Length of hospital stay (days), median (25th–75th percentile)	78 (65.5–95.5)	5 (4–6)
Age at 7-year scan (years), mean (SD)	7.5 (0.2)	7.6 (0.2)
WASI IQ, mean (SD)	99.1 (13.0)	109.5 (11.4)
Movement ABC-2 total standardized score, mean (SD)	9.0 (3.2)[d]	11.2 (2.7)[e]
WRAT4 Math computation, mean (SD)	91.5 (17.4)[b]	98.7 (14.5)
WRAT4 Reading, mean (SD)	100.4 (18.3)[b]	108.6 (17.8)
SDQ total score, mean (SD)	9.9 (6.4)[f]	6.8 (5.2)[g]

Movement ABC-2, Movement Assessment Battery for Children-2nd Edition; SD, standard deviation; SDQ, Strengths and Difficulties Questionnaire; VPT, very preterm; WASI, Wechsler Abbreviated Scale of Intelligence; WRAT4, Wide Range Achievement Test 4th Edition.
[a] $n = 141$.
[b] $n = 144$.
[c] Proven sepsis and/or necrotizing enterocolitis.
[d] $n = 137$.
[e] $n = 32$.
[f] $n = 138$.
[g] $n = 30$.

compared with controls in the same tracts as the original analysis (data not shown).

Perinatal Predictors in the VPT Group

GA at birth

There were several voxels where GA at birth correlated positively with FA in VPT children, located within the fiber tracts listed in Table IV. These correlations between GA at birth and FA disappeared when birthweight SD score and neonatal brain abnormality were included in the model. There were no voxels where GA at birth correlated with axon dispersion or density in VPT children.

Birthweight SD score

There were no voxels where birthweight SD score correlated with FA, axon dispersion, or axon density in VPT children.

Neonatal brain abnormality

There were many voxels where neonatal brain abnormality scores correlated negatively with FA in VPT children, encompassing many major fiber tracts (Table IV, Fig. 4A). There were also many voxels where neonatal brain abnormality scores correlated positively with axon dispersion in VPT children; these voxels were generally co-located within the same fiber tracts as the voxels where neonatal brain abnormality scores correlated with FA (Table IV, Fig. 4B). There were no voxels where neonatal brain abnormality scores correlated in the opposing directions to those stated with FA or axon dispersion. Analogous results were found when GA at birth and birthweight SD score were included in the models. However, the correlations between neonatal brain abnormality scores and axon dispersion disappeared when the participants whose $b = 3{,}000$ s/mm^2 diffusion images were acquired with non-uniform gradient directions were excluded from the analyses. There were no voxels where neonatal brain abnormality scores correlated with axon density in VPT children.

Correlations with Neurodevelopmental Outcomes in the VPT Group

IQ

There were many voxels where FA correlated positively with IQ in VPT children, located within most major fiber

TABLE II. Very preterm (VPT) children vs. controls

	FA	Axon dispersion	Axon density
Direction of group differences	VPT < Controls	VPT > Controls	No differences
Total number of voxels (% skeleton)	227 (0.1)	43,793 (22)	N/A
White matter tracts	Cingulum (hippocampal part) R	Cingulum (gyral and hippocampal parts)	N/A
	Inferior longitudinal fasciculus R	Inferior longitudinal fasciculus	
	Inferior fronto-occipital fasciculus R	Inferior fronto-occipital fasciculus	
	Uncinate fasciculus R	Uncinate fasciculus	
	Anterior thalamic radiation R	Anterior thalamic radiation	
	External capsule R	External capsule	
		Internal capsule (anterior limb, posterior limb, retrolenticular part)	
		Corticospinal tract	
		Superior longitudinal fasciculus (including temporal part)	
		Corpus callosum (body, genu, splenium)	
		Forceps major and minor	
		Cerebellar peduncle (middle, inferior, superior, pontine crossing tract)	
		Fornix (column and body, cres/stria terminalis)	
		Posterior thalamic and optic radiation	
		Corona radiata (anterior, posterior, superior)	
		Cerebral peduncle	
		Medial lemniscus	
		Superior fronto-occipital fasciculus	
		Sagittal stratum	

FA, fractional anisotropy. Significant regions were located in both the left (L) and right (R) hemispheres of the brain unless otherwise stated.

tracts (Table V, Fig. 5A). There were also many voxels where axon density correlated positively with IQ in VPT children, which were co-located within many of the same tracts as the correlations between FA and IQ (Table V, Fig. 5B). When the participants whose $b = 3{,}000$ s/mm^2 diffusion images were acquired with non-uniform gradient directions were excluded from the analyses, there remained many voxels where axon density correlated positively with IQ in VPT children, although these voxels became less widespread across the white matter (Supporting Information Table I, Supporting Information Fig. 1B). There were no voxels where axon dispersion correlated with IQ in VPT children.

Motor function

FA correlated positively with motor scores within most major fiber tracts in VPT children (Table V, Fig. 6A). Additionally, there were many voxels where axon dispersion correlated negatively with motor scores in VPT children. These voxels were co-located within most of the same tracts as the correlations between FA and motor scores, although they were somewhat less extensive over the white matter skeleton (Table V, Fig. 6B). There were also many voxels where axon density correlated positively with motor scores in VPT children, again co-located within many of the same tracts as the correlations between FA and motor scores, although they were spread less extensively across the skeleton (Table V, Fig. 6C). When the participants whose $b = 3{,}000$ s/mm^2 diffusion images were acquired with non-uniform gradient directions were excluded from the analyses, the correlations between axon dispersion and motor scores disappeared; however, the correlations between axon density and motor scores became more widespread (Supporting Information Table I; Supporting Information Fig. 1C).

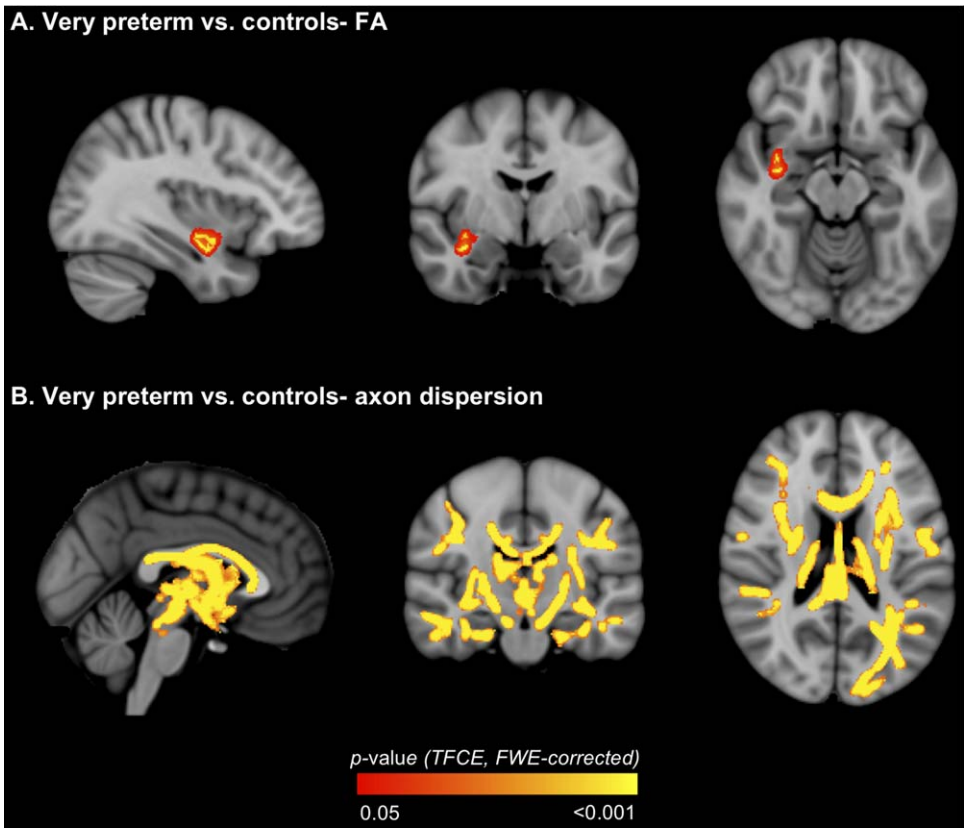

Figure 2.

Regions where white matter diffusion values [**A**. fractional anisotropy (FA); **B**. axon dispersion] differed between the very preterm and control groups. The *P*-value images, displayed in *red-yellow*, have been thickened for visualization and overlaid on the standard space (MNI152) T_1-weighted image. Only $P < 0.05$, after threshold-free cluster enhancement (TFCE) and correction for the family-wise error rate (FWE), are shown. [Color figure can be viewed in the online issue, which is available at wileyonlinelibrary.com.]

Academic performance

FA within many widespread fiber tracts correlated positively with math computation and reading scores in VPT children (Table V, Fig. 7A and B, respectively). There were no voxels where axon dispersion or axon density correlated with math computation or reading scores in VPT children.

Behavioral/emotional problems

FA in most major fiber tracts correlated negatively with behavioral/emotional scores in VPT children (Table V, Fig. 8A). There were also many voxels where axon density correlated negatively with behavioral/emotional scores in VPT children, which were co-located within most of the same fiber tracts as the correlations between FA and behavioral/emotional scores (Table V, Fig. 8B). Axon dispersion also correlated positively with behavioral/emotional scores in VPT children; these correlations were restricted to a small area (Table V, Fig. 8C). The correlations between axon density and axon dispersion and behavioral/emotional scores were similar when the participants whose $b = 3{,}000$ s/mm^2 diffusion images were acquired with non-uniform gradient directions were excluded from the analyses (data not shown).

DISCUSSION

Summary

Applying DTI and NODDI to study brain white matter microstructure in VPT children and controls, we found: (1) lower FA and higher axon dispersion, but no difference in axon density, in major white matter tracts in VPT children; (2) significant associations between neonatal brain abnormality and lower FA and higher axon dispersion in widespread tracts in VPT children; (3) significant associations between FA, axon dispersion and axon density in various tracts and neurodevelopmental outcomes in VPT children.

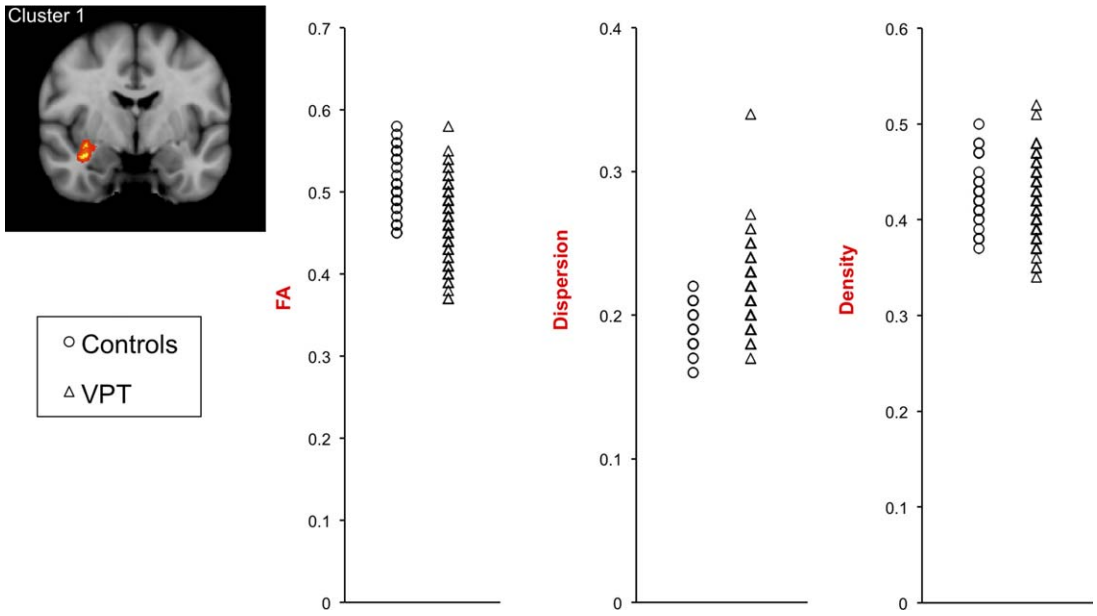

Figure 3.

Scatterplots of fractional anisotropy (FA), axon dispersion and axon density values in the very preterm (VPT) and control groups. The values are averaged from within the cluster of voxels in which FA was significantly lower in the VPT group compared with controls ($P < 0.05$, after threshold-free cluster enhancement and correction for the family-wise error rate). [Color figure can be viewed in the online issue, which is available at wileyonlinelibrary.com.]

VPT Children Compared with Controls

VPT children had a cluster of lower FA compared with controls. Despite the difficulties in interpreting FA due to its low biological specificity, FA is generally considered a useful biomarker of the overall microstructural organization and coherency of brain white matter [Jones et al., 2013]. In white matter, FA increases with age in typical development, and is higher in the early maturing white matter tracts such as the internal capsule and corpus callosum compared with later maturing white matter tracts [Mukherjee and McKinstry, 2006]. This suggests that lower FA in white matter in VPT children reflects delayed and/or disrupted white matter development. Several previous studies that compared FA between preterm children/adolescents and term-born controls using whole brain methods such as TBSS found that FA is lower in the preterm groups in many white matter tracts [Allin et al., 2011; Eikenes et al., 2011; Skranes et al., 2007; Vangberg et al., 2006], however some studies found no FA group differences [Feldman et al., 2012; Loe et al., 2013]. For the studies that found lower FA, this was located in some of the same white matter tracts as the current study, including the cingulum [Eikenes et al., 2011], external capsule [Eikenes et al., 2011; Skranes et al., 2007], inferior fronto-occipital/longitudinal fasciculus [Eikenes et al., 2011; Skranes et al., 2007], uncinate fasciculus [Eikenes et al., 2011], and thalamic region [Eikenes et al., 2011]. Lower FA was also reported previously in the corpus callosum [Allin et al., 2011; Eikenes et al., 2011; Skranes et al., 2007; Vangberg et al., 2006], internal capsule [Skranes et al., 2007; Vangberg et al., 2006], superior longitudinal fasciculus [Allin et al., 2011; Eikenes et al., 2011; Skranes et al., 2007], corona radiata [Allin et al., 2011; Eikenes et al., 2011], and

TABLE III. Diffusion values in the very preterm (VPT) and control groups

Diffusion measure	Controls, mean (SD)	VPT, mean (SD)	Mean difference (95% CI)	*P*
FA	0.51 (0.04)	0.46 (0.04)	−0.04 (−0.06, −0.03)	<0.001
Dispersion	0.19 (0.02)	0.21 (0.02)	0.02 (0.02, 0.03)	<0.001
Density	0.43 (0.03)	0.42 (0.03)	−0.007 (−0.02, 0.006)	0.3

The values are averaged from within the cluster of voxels where fractional anisotropy (FA) was significantly lower in the VPT group compared with controls ($P < 0.05$, after threshold-free cluster enhancement and correction for the family-wise error rate). CI, confidence interval; SD, standard deviation.

TABLE IV. Perinatal predictors in the very preterm group

		FA	Axon dispersion	Axon density
GA at birth	**Direction of correlations**	Positive	No correlations	No correlations
	Total number of voxels (% skeleton)	2,317 (1)	N/A	N/A
	White matter tracts	Cerebral peduncle L Corticospinal tract L Inferior fronto-occipital fasciculuis Inferior longitudinal fasciculus Uncinate fasciculus Anterior thalamic radiation Internal capsule (anterior limb, posterior limb, retrolenticular part L) Forceps minor Cingulum (hippocampal part R) Fornix (cres/stria terminalis L) Superior longitudinal fasciculus (including temporal part) Corona radiata (anterior) External capsule Sagittal stratum	N/A	N/A
Birthweight SD Score	**Direction of correlations**	No correlations	No correlations	No correlations
	Total number of voxels (% skeleton)	N/A	N/A	N/A
	White matter tracts	N/A	N/A	N/A
Neonatal brain abnormality	**Direction of correlations**	Negative	Positive	No correlations
	Total number of voxels (% skeleton)	17,546 (9)	7,589 (4)	N/A
	White matter tracts	Corticospinal tract Inferior fronto-occipital fasciculus Inferior longitudinal fasciculus Uncinate fasciculus Anterior thalamic radiation Internal capsule (posterior limb and retrolenticular part) Corpus callosum (body, genu, splenium) Forceps minor and major Cingulum (gyral and hippocampal parts) Fornix (column and body, cres/stria terminalis) Posterior thalamic and optic radiation Superior longitudinal fasciculus (including temporal part) Corona radiata (anterior, superior, posterior) Tapetum R Cerebral peduncle External capsule R	Corticospinal tract Inferior fronto-occipital fasciculus Inferior longitudinal fasciculus Uncinate fasciculus Anterior thalamic radiation Internal capsule (retrolenticular part R) Corpus callosum (body, genu, splenium) Forceps minor and major Cingulum (gyral and hippocampal parts) Fornix (column and body, cres/stria terminalis) Posterior thalamic and optic radiation Superior longitudinal fasciculus (including temporal part) Corona radiata (anterior, superior, posterior) Tapetum R Sagittal stratum L	

FA, fractional anisotropy; GA, gestational age; SD, standard deviation. Significant regions were located in both the left (L) and right (R) hemispheres of the brain unless otherwise stated.

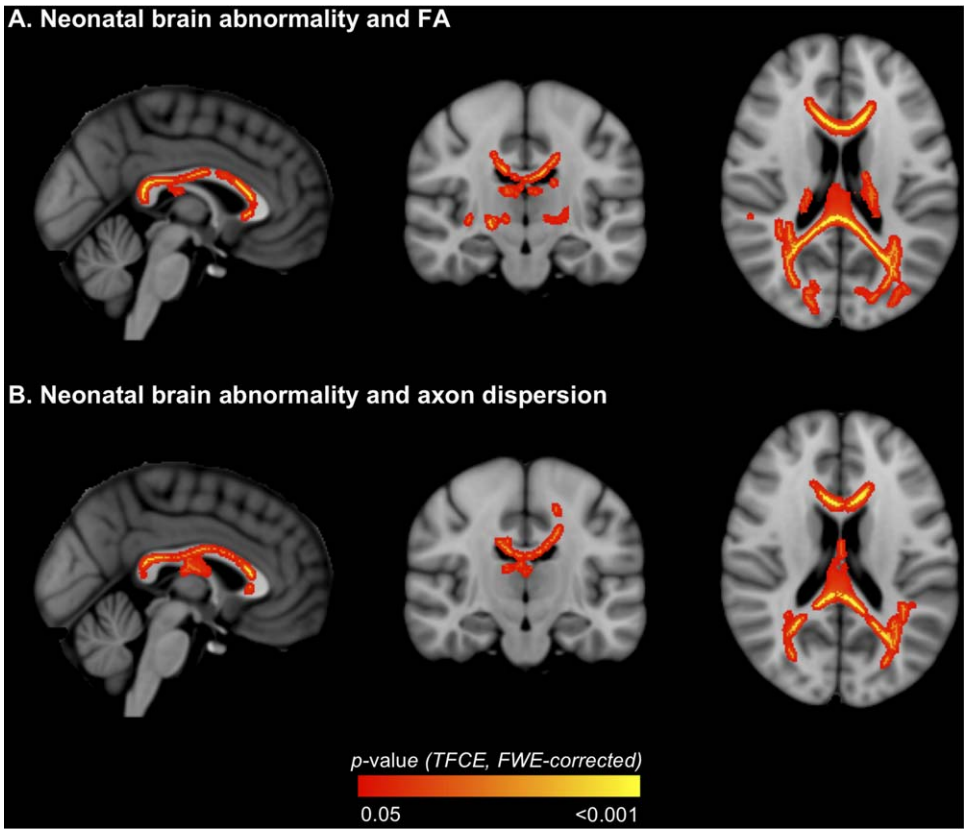

Figure 4.

Regions where neonatal brain abnormality correlated with white matter diffusion values [A. fractional anisotropy (FA); B. axon dispersion] in very preterm children. The *P*-value images, displayed in *red-yellow*, have been thickened for visualization and overlaid on the standard space (MNI152) T_1-weighted image. Only $P < 0.05$, after threshold-free cluster enhancement (TFCE) and correction for the family-wise error rate (FWE), are shown. [Color figure can be viewed in the online issue, which is available at wileyonlinelibrary.com.]

occipital white matter/optic radiation [Eikenes et al., 2011; Vangberg et al., 2006], which the current study surprisingly did not find. Discrepancies between studies are likely due to different sample characteristics and imaging methods. The studies that reported lower FA were older studies including participants born in the 1980s [Allin et al., 2011; Eikenes et al., 2011; Skranes et al., 2007; Vangberg et al., 2006], for example, the studies by Vangberg, Skranes, and Eikenes were based on the same cohort born between 1986 and 1988, whereas the studies that did not find FA differences included participants born in the 1990s [Feldman et al., 2012; Loe et al., 2013], and the current study included participants born in the early 2000s. Neonatal intensive care has greatly improved over time, particularly with the introduction of surfactant treatment in 1991 and increased use of antenatal corticosteroids [Doyle, 2004], which may influence white matter microstructural development. Rates of major neonatal brain injury may also influence FA group differences in childhood. The studies by Feldman et al. and Loe et al. included children who had low levels of neonatal brain injury, which the authors postulated may explain their lack of FA group differences [Feldman et al., 2012; Loe et al., 2013]. Unfortunately rates of neonatal brain injury were not reported in all previous studies [Allin et al., 2011; Eikenes et al., 2011; Skranes et al., 2007; Vangberg et al., 2006]. Rates of major neonatal brain injury were relatively low (~5%) in the current study (Table I). Furthermore, VPT participants had slightly lower neonatal brain abnormality scores than VPT non-participants, and so FA group differences may have been stronger if all participants had been included. The current study included 7-year-old children, whereas the previous studies included older children or adolescents (9–16 years [Feldman et al., 2012; Loe et al., 2013]; 15 years [Skranes et al., 2007; Vangberg et al., 2006]; 18–22 years [Eikenes et al., 2011]; 17–22 years [Allin et al., 2011]), and FA group differences may vary from childhood to early adulthood, although this is yet to be investigated in

TABLE V. Correlations with neurodevelopmental outcomes in the very preterm group

		FA	Axon dispersion	Axon density
IQ	**Direction of correlations**	Positive	No correlations	Positive
	Total number of voxels (% skeleton)	52,375 (27)	N/A	19,049 (10)
	White matter tracts	Cerebellar peduncle (middle, inferior, superior, pontine crossing tract) Cerebral peduncle Corticospinal tract Inferior fronto-occipital fasciculus Inferior longitudinal fasciculus Uncinate fasciculus Anterior thalamic radiation External capsule Internal capsule (anterior limb, posterior limb, retrolenticular part) Corpus callosum (body, genu, splenium) Forceps major and minor Cingulum (gyral and hippocampal parts) Fornix (cres/stria terminalis) Posterior thalamic and optic radiation Superior longitudinal fasciculus (including temporal part) Corona radiata (anterior, superior, posterior) Sagittal stratum Superior fronto-occipital fasciculus L Medial lemniscus Tapetum R	N/A	Cerebellar peduncle (middle, inferior R, superior) Cerebral peduncle Corticospinal tract Inferior fronto-occipital fasciculus Inferior longitudinal fasciculus L Uncinate fasciculus Anterior thalamic radiation External capsule Internal capsule (anterior limb, posterior limb, retrolenticular part L) Corpus callosum (body, splenium) Forceps major and minor Cingulum (gyral part, hippocampal part L) Fornix (column and body, cres/stria terminalis L) Posterior thalamic and optic radiation L Superior longitudinal fasciciulus (including temporal part) Corona radiata (anterior, superior, posterior) Sagittal stratum L Superior fronto-occipital fasciculus R
Motor function	**Direction of correlations**	Positive	Negative	Positive
	Total number of voxels (% skeleton)	77,813 (40)	17,495 (9)	7,528 (4)
	White matter tracts	Cerebellar peduncle (middle, inferior, superior, pontine crossing tract) Corticospinal tract Inferior fronto-occipital fasciculus Inferior longitudinal fasciculus Uncinate fasciculus Anterior thalamic radiation Internal capsule (anterior limb, posterior limb, retrolenticular part)	Cerebellar peduncle (superior L) Corticospinal tract Inferior fronto-occipital fasciculus Inferior longitudinal fasciculus Uncinate fasciculus Anterior thalamic radiation Internal capsule (anterior limb, posterior limb, retrolenticular part)	Cerebellar peduncle (middle) Corticospinal tract Inferior fronto-occipital fasciculus Inferior longitudinal fasciculus Uncinate fasciculus R Anterior thalamic radiation Internal capsule (anterior limb, posterior limb, retrolenticular part)

TABLE V. (continued).

		FA	Axon dispersion	Axon density
		Corpus callosum (body, genu, splenium) Forceps major and minor Cingulum (gyral and hippocampal parts) Fornix (column and body, cres/stria terminalis) Posterior thalamic and optic radiation Superior longitudinal fasciculus (including temporal part) Corona radiata (anterior, superior, posterior) Tapetum R External capsule Cerebral peduncle Sagittal stratum Superior fronto-occipital fasciculus R Medial lemniscus	Corpus callosum (body, genu, splenium) Forceps major and minor Cingulum (gyral and hippocampal parts) Fornix (column and body, cres/stria terminalis) Posterior thalamic and optic radiation Superior longitudinal fasciculus (including temporal part) Corona radiata (anterior, superior, posterior) Tapetum R External capsule Cerebral peduncle Sagittal stratum R Superior fronto-occipital fasciculus R	Corpus callosum (body, splenium) Forceps major and minor Cingulum (gyral and hippocampal parts) Fornix (column and body, cres/stria terminalis) Posterior thalamic and optic radiation Superior longitudinal fasciculus (including temporal part) Corona radiata (superior, posterior) Tapetum R
Academic performance	**Direction of correlations**	Positive	No correlations	No correlations
	Total number of voxels (% skeleton)	Math 56,350 (29); Reading 18,947 (10)	N/A	N/A
	White matter tracts	Cerebellar peduncle (middle, inferior, superior, pontine crossing tract) Cerebral peduncle Corticospinal tract Inferior fronto-occipital fasciculus Inferior longitudinal fasciculus Uncinate fasciculus Anterior thalamic radiation External capsule Internal capsule (anterior limb, posterior limb, retrolenticular part) Corpus callosum (body, genu, splenium maths only) Forceps major and minor Cingulum (gyral and hippocampal part) Fornix (column and body, cres/stria terminalis) Posterior thalamic and optic radiation Superior longitudinal fasciculus (including temporal part)	N/A	N/A

TABLE V. (continued).

		FA	Axon dispersion	Axon density
		Corona radiata (anterior, superior, posterior) Medial lemniscus Sagittal stratum Tapetum R Superior fronto-occipital fasciculus L (reading only)		
Behavioral/ emotional problems	**Direction of correlations**	Negative	Positive	Negative
	Total number of voxels (% skeleton)	61,907 (32)	74 (0.04)	55,541 (29)
	White matter tracts	Corpus callosum (body, genu, splenium) Forceps major and minor Cerebral peduncle Corticospinal tract Inferior fronto-occipital fasciculus Inferior longitudinal fasciculus Uncinate fasciculus Anterior thalamic radiation External capsule Internal capsule (anterior limb, posterior limb, retrolenticular part) Cingulum (gyral and hippocampal parts) Fornix (column and body, cres/stria terminalis) Posterior thalamic and optic radiation Superior longitudinal fasciculus (including temporal part) Corona radiata (anterior, superior, posterior) Sagittal stratum Superior fronto-occipital fasciculus R Tapetum R Cerebellar peduncle (middle, inferior, superior, pontine crossing tract) Medial lemniscus L	Corpus callosum (body and genu) Forceps minor	Corpus callosum (body, genu, splenium) Forceps major and minor Cerebral peduncle L Corticospinal tract Inferior fronto-occipital fasciculus Inferior longitudinal fasciculus Uncinate fasciculus Anterior thalamic radiation External capsule Internal capsule (anterior limb, posterior limb, retrolenticular part) Cingulum (gyral and hippocampal parts) Fornix (cres/stria terminalis) Posterior thalamic and optic radiation Superior longitudinal fasciculus (including temporal part) Corona radiata (anterior, superior, posterior) Sagittal stratum Superior fronto-occipital fasciculus Tapetum R

FA, fractional anisotropy. Significant regions were located in both the left (L) and right (R) hemispheres of the brain unless otherwise stated.

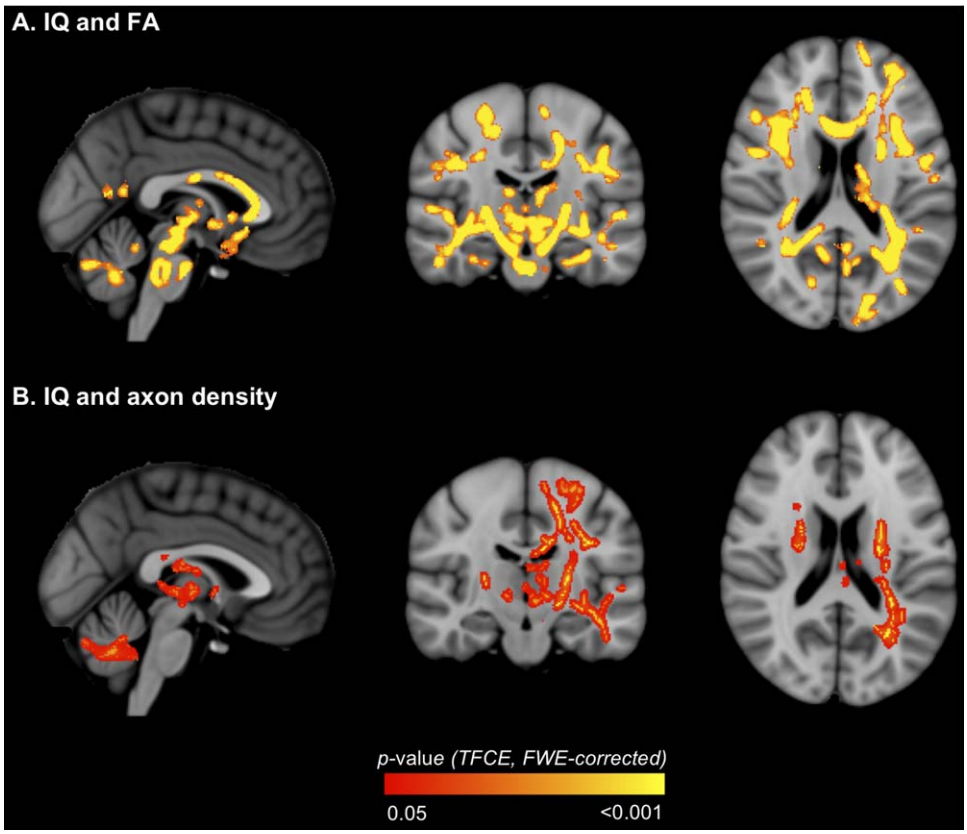

Figure 5.

Regions where white matter diffusion values [A. fractional anisotropy (FA); B. axon density] in very preterm children correlated with IQ. The *P*-value images, displayed in *red-yellow*, have been thickened for visualization and overlaid on the standard space (MNI152) T_1-weighted image. Only $P < 0.05$, after threshold-free cluster enhancement (TFCE) and correction for the family-wise error rate (FWE), are shown. [Color figure can be viewed in the online issue, which is available at wileyonlinelibrary.com.]

longitudinal cohorts using whole brain methods. Several previous studies used voxel-based morphometry (VBM) rather than TBSS [Allin et al., 2011; Skranes et al., 2007; Vangberg et al., 2006]. Unlike TBSS, VBM does not restrict analyses to a white matter skeleton, and so results obtained using VBM are likely to be more influenced by partial voluming [Bach et al., 2014; Smith et al., 2006]. On the other hand, the skeletonization step in TBSS restricts analyses to regions with FA above a certain value (typically 0.2 as in the current study), which generally corresponds to the centers of major white matter tracts, and so FA differences may be missed in regions with lower FA such as at the tract perimeter when using TBSS [Bach et al., 2014].

Given the low biological specificity of DTI, lower FA in VPT children could be due to changes in numerous white matter microstructural properties, including axon density, axon diameter, membrane permeability, myelination, and axon orientation distributions [Jones et al., 2013]. Further analysis with NODDI provided increased biological specificity by disentangling two key factors potentially contributing to FA changes within white matter, the axon density, and axon dispersion [Zhang et al., 2012]. Using NODDI, the current study found that VPT children had increased axon dispersion in many white matter tracts compared with controls, including within those tracts in which FA was lower in VPT children, while there was no significant difference in axon density between groups. This suggests that low FA in VPT children in certain white matter tracts is due at least in part to increases in axon dispersion. Furthermore the current results suggest that NODDI may be even more sensitive to detecting group differences than FA, given that many more tracts were found to have increased dispersion compared with the tracts found to have lower FA. Within the adult brain, dispersion values are relatively low in the white matter (compared with other brain tissue types, i.e., gray matter and CSF), which is due to the presence of axons that are generally

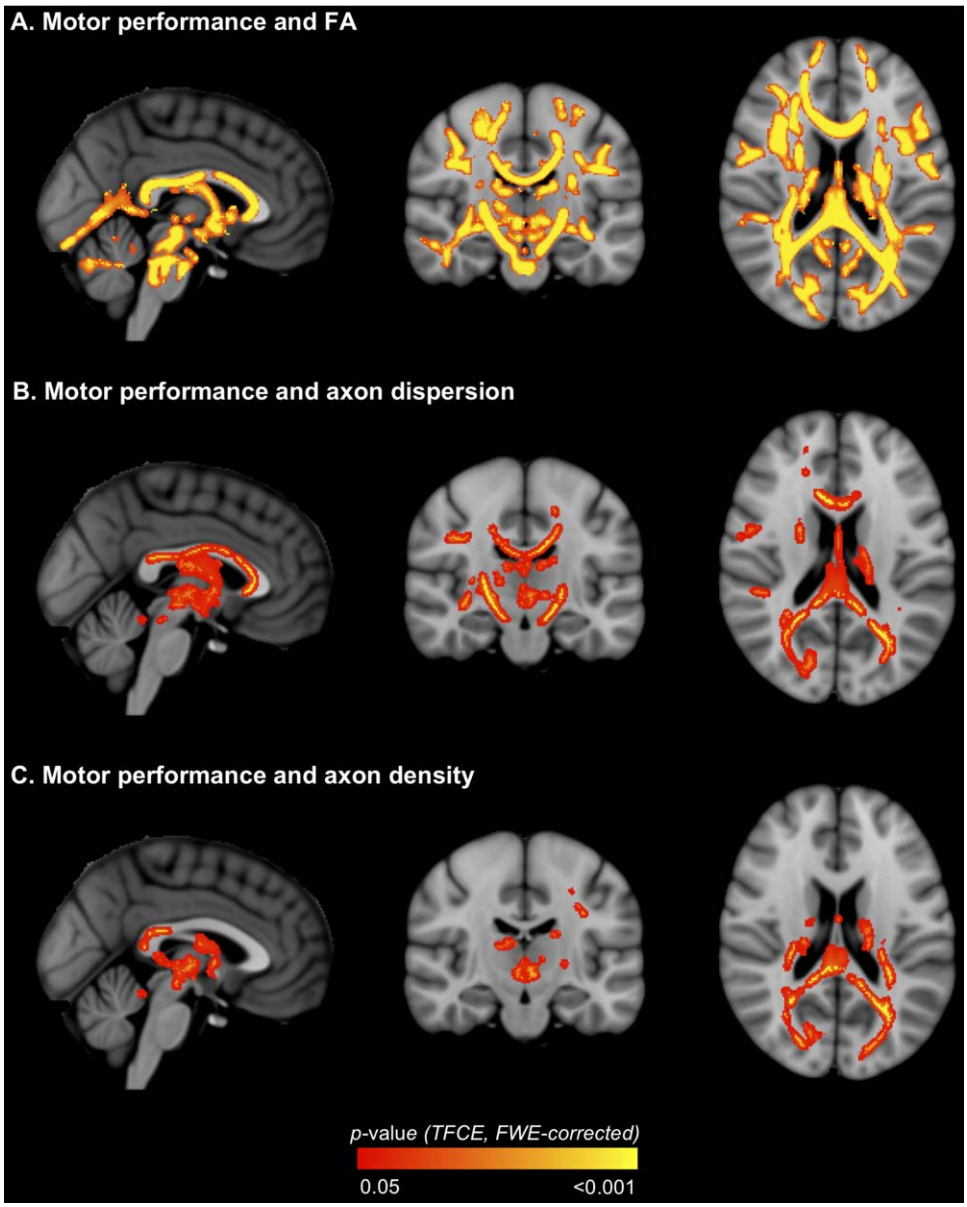

Figure 6.

Regions where white matter diffusion values [A. fractional anisotropy (FA); B. axon dispersion; C. axon density] in very preterm children correlated with motor scores. The *P*-value images, displayed in red-yellow, have been thickened for visualization and overlaid on the standard space (MNI152) T_1-weighted image. Only $P < 0.05$, after threshold-free cluster enhancement (TFCE) and correction for the family-wise error rate (FWE), are shown. [Color figure can be viewed in the online issue, which is available at wileyonlinelibrary.com.]

coherently oriented and aligned [Zhang et al., 2012]. Within the white matter itself, the lowest dispersion values are found in tracts that have more coherently oriented and organized axons such as the corpus callosum and internal capsule, while the highest dispersion values are found in tracts that have less coherently organized axons (more bending and fanning axons) such as the centrum semiovale [Zhang et al., 2012]. Therefore, it is possible that when comparing VPT children with controls, higher axon dispersion in many of the major white matter tracts may be less favorable as it may indicate a reduction in the normal coherent organization of axons.

The original NODDI study showed that FA and axon dispersion are strongly inversely correlated with each

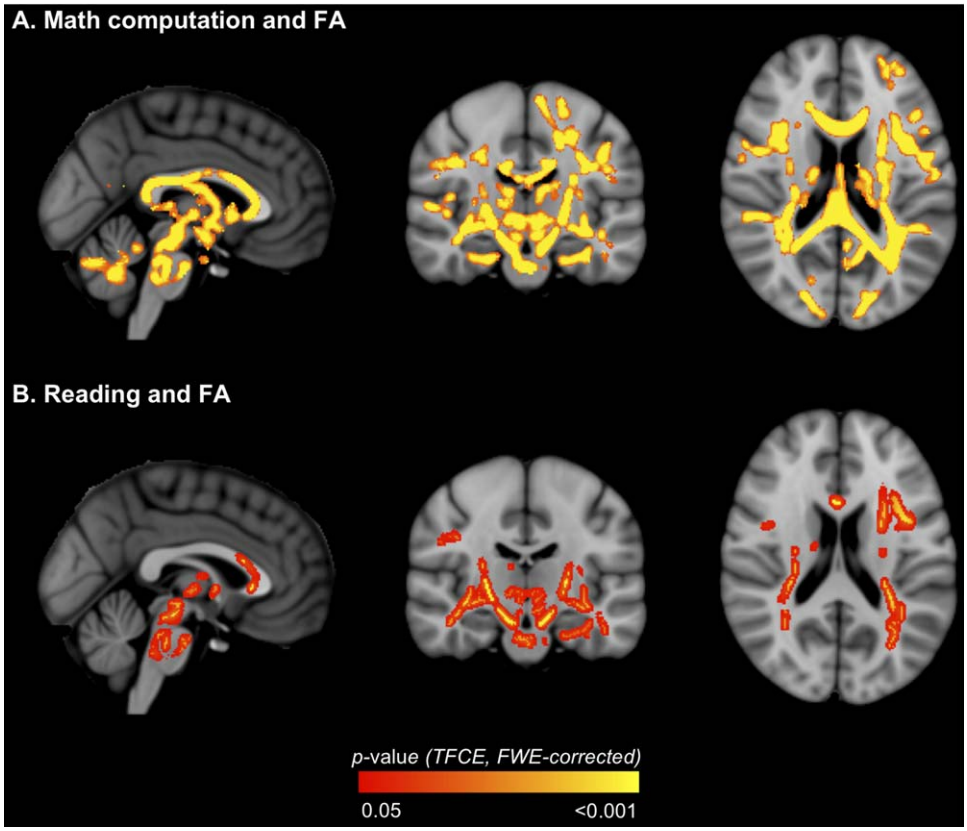

Figure 7.

Regions where fractional anisotropy (FA) in very preterm children correlated with academic outcomes [A. math computation; B. reading]. The *P*-value images, displayed in *red-yellow*, have been thickened for visualization and overlaid on the standard space (MNI152) T_1-weighted image. Only $P < 0.05$, after threshold-free cluster enhancement (TFCE) and correction for the family-wise error rate (FWE), are shown. [Color figure can be viewed in the online issue, which is available at wileyonlinelibrary.com.]

other (i.e., the lowest values of axon dispersion within the most coherently organized white matter tracts correspond to the highest values of FA) [Zhang et al., 2012]. Additionally, in the original NODDI paper axon density showed a weaker positive correlation with FA, suggesting that FA is more sensitive to axon dispersion than axon density [Zhang et al., 2012]. This is similar to the results of the current study, in which we found that the areas of decreased FA in the VPT group corresponded with increased axon dispersion, but not density. NODDI has not been applied previously to study brain white matter in preterm cohorts, although studies have applied NODDI to the developing neonatal brain white matter [Kunz et al., 2014; Melbourne et al., 2013]. These studies reported that NODDI parameters could distinguish early from later maturing fiber tracts in the neonatal period; for example, the partially myelinated posterior limb of the internal capsule had lower dispersion and higher density compared with the non-myelinated anterior limb of the internal capsule [Kunz et al., 2014]. This finding supports the interpretation that higher dispersion values observed in VPT children in the current study reflect altered and/or delayed white matter maturation. Other applications of NODDI include patients with specific genetic variants (16p11.2 deletions) [Owen et al., 2014], neurofibromatosis [Billiet et al., 2014], and classic galactosemia [Timmers et al., 2015]. In all of these previous studies, NODDI was able to provide more detailed information regarding brain white matter microstructure changes than FA alone. NODDI has also recently been used to study *gray matter* (cortical and thalamic) microstructure in preterm infants shortly after birth and at term-equivalent age [Eaton-Rosen et al., 2015].

As a secondary analysis, we showed that the group differences in FA and axon dispersion persisted when VPT children who had IVH grade 3/4 and/or cystic PVL in the neonatal period were excluded. This finding indicates that the group differences were not restricted to VPT children

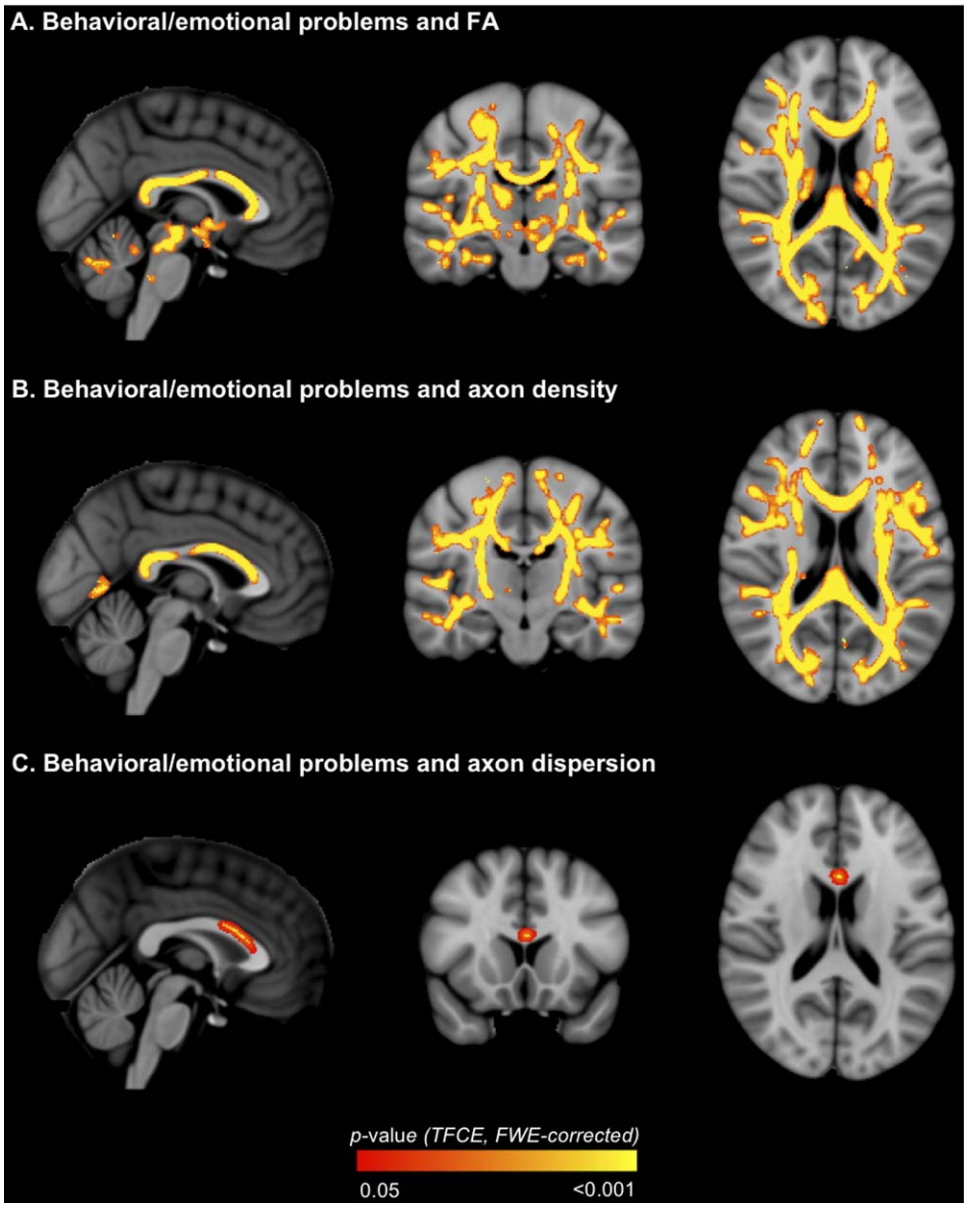

Figure 8.

Regions where white matter diffusion values [A. fractional anisotropy (FA); B. axon density; C. axon dispersion] in very preterm children correlated with behavioral/emotional outcome. The *P*-value images, displayed in *red-yellow*, have been thickened for visualization and overlaid on the standard space (MNI152) T_1-weighted image. Only $P < 0.05$, after threshold-free cluster enhancement (TFCE) and correction for the family-wise error rate (FWE), are shown. [Color figure can be viewed in the online issue, which is available at wileyonlinelibrary.com.]

with major brain injury. Additionally, to further aid the reader in interpreting the current FA and NODDI results, we provided axial, radial, and mean diffusivity values for the VPT and control groups. Within the region in which FA was lower in the VPT children compared with controls, axial diffusivity was lower and radial and mean diffusivities were higher. This is similar to previous studies of DTI values in various white matter tracts in the same cohort as the current study, in which we have shown that white matter radial and mean diffusivities are increased in the VPT group compared with controls [Murray et al., 2015; Thompson et al., 2015, 2014b]. However, similar to

FA, the biological interpretation of changes in the diffusivities is unclear; therefore, it is important to use techniques such as NODDI, which provides greater biological specificity compared with DTI.

Perinatal Predictors

GA at birth predicted lower FA in VPT children, although this finding disappeared after adjusting for birthweight SD score and neonatal brain abnormalities, suggesting that GA at birth is not an independent predictor of white matter microstructure at age 7 years. Neonatal brain abnormalities predicted lower FA and increased axon dispersion in VPT children in widespread tracts, independent of GA at birth and birthweight SD score. This suggests that VPT children who had neonatal brain abnormalities tend to have less coherently organized axons. Previous studies have found associations between neonatal brain injury and later white matter DTI values. Feldman et al. found that neonatal white matter injury was associated with lower FA in childhood, particularly in the corpus callosum and the posterior and periventricular white matter [Feldman et al., 2012]. Allin et al. reported differences in white matter FA between adolescents who did and did not have abnormalities on neonatal ultrasound (periventricular hemorrhage and ventricular dilation) [Allin et al., 2011]. We have also previously shown that neonatal brain abnormality is associated with widespread lower FA and increased diffusivities in infancy in the same cohort as the current study [Thompson et al., 2014a]. The current study builds on previous studies, suggesting that correlations between neonatal brain abnormalities and white matter DTI values could reflect changes in axon dispersion.

Neurodevelopmental Outcomes

The results suggested that FA and NODDI parameters have functional significance in VPT children, detecting structure-function relationships with several key neurodevelopmental outcomes. Lower FA in widespread white matter tracts was associated with poorer IQ, while lower axon density in many of the same tracts was also associated with poorer IQ. This suggests that associations between low FA and poorer IQ are related to decreases in axon density. Lower axon density may reflect axon loss and/or increased space between axons [Billiet et al., 2014]. Additionally, axon density may be a useful marker for myelination, as it correlates strongly with the intensity of myelin stain under light microscopy [Jespersen et al., 2010]. Similar to the current study, previous studies that have used whole brain methods have also found associations between FA in widespread tracts and IQ in preterm children or adolescents [Allin et al., 2011; Eikenes et al., 2011; Feldman et al., 2012; Skranes et al., 2007]. White matter tracts consistently identified as being associated with IQ include the inferior fronto-occipital, inferior longitudinal, superior longitudinal and uncinate fasciculi, and the corpus callosum/forceps minor, which were also found to be associated with IQ in the current study [Allin et al., 2011; Eikenes et al., 2011; Feldman et al., 2012; Skranes et al., 2007].

Lower FA in widespread tracts was also associated with poorer motor outcome, while in many of the same tracts lower axon density and higher axon dispersion were associated with poorer motor outcome. The correlations between motor scores and FA, dispersion and density were generally co-located in the same tracts. However, there were some tracts in which motor scores were related to FA and axon dispersion, but not to axon density; the corpus callosum genu, left uncinate fasciculus, external capsule, cerebral peduncle, right sagittal stratum, and right superior fronto-occipital fasciculus. This supports the ability of NODDI to disentangle the factors contributing to FA in particular white matter regions. Overall the associations between FA, axon dispersion and axon density and motor outcome in VPT children were widespread, and included fiber tracts known to be important for motor functioning, such as the corticospinal tract, the posterior limb of the internal capsule and cerebral peduncle (regions that the corticospinal tract fibers pass through), the corpus callosum body (which interconnects the motor cortical areas), and the corona radiata (which contains projectional motor fibers) [Duvernoy, 1999]. Similarly, several previous studies have found that reduced FA in various white matter pathways, particularly the corticospinal tract, and also the corpus callosum, is associated with motor delays in children born preterm [de Kieviet et al., 2014; Groeschel et al., 2014; Lee et al., 2011; Skranes et al., 2007; Thompson et al., 2015].

Additionally, worse behavioral/emotional outcome was associated with poorer white matter microstructural organization, including lower FA and axon density in widespread tracts, as well as higher axon dispersion in the corpus callosum/forceps minor. This is a relatively novel finding, as only a few previous studies have also found that lower FA in widely distributed tracts is associated with behavioral and emotional problems in preterm children, including attention and internalizing behavior problems [Loe et al., 2013], and mild social deficits, inattention symptoms, and attention-deficit hyperactivity disorder [Skranes et al., 2007].

LIMITATIONS

We applied NODDI retrospectively to multi-shell diffusion images acquired with different acquisition parameters (e.g., different TEs, TRs and voxel sizes between diffusion shells), in line with previous studies [Counsell et al., 2014; Owen et al., 2014]. However, we acknowledge that this is a limitation of our study and our results should be interpreted with caution given this limitation. Future studies with equivalent acquisition parameters for all diffusion

shells are required to validate our results. It is possible that the different acquisition parameters between diffusion shells may cause the neurite density maps to show a weaker contrast between gray matter and white matter than is usually seen in NODDI maps (Fig. 1). It is also possible that the different acquisition parameters between shells may explain the fact that no differences in axon density were found between the VPT children and controls, which was contrary to our original hypothesis. While we have attempted to mitigate the effects of the different voxel sizes, TEs and TRs between diffusion shells by resampling the shells to the same resolution and normalizing each shell by its $b = 0$ s/mm^2 volume, we acknowledge that these correction steps do not compensate for all possible differences between the shells, including differences in gradient pulse width and separation and differences in the amounts of partial voluming.

TBSS has several limitations that could complicate interpretation of our findings [Bach et al., 2014]. The skeletonization step may limit the reliability of the final results as it introduces a spatial variability and orientational heterogeneity of the statistical sensitivity [Edden and Jones, 2011]. An additional drawback of confining the spatial location of the analysis to a skeleton is the lack of specificity [Jones and Cercignani, 2010]. In regions where multiple fiber structures converge, such as the interface of the superior parts of the corpus callosum and the corticospinal tracts, the skeleton cannot be defined unambiguously [Van Hecke et al., 2010]. Recent work suggests that using more advanced registration methods improves cross-subject alignment [Schwarz et al., 2014; Van Hecke et al., 2007], increasing reliability of statistical inferences.

Another potential limitation of our study was the inclusion of a non-uniform gradient scheme for the b-value = 3,000 s/mm^2 diffusion data in 29% of our VPT sample and 27% of our control sample, which may introduce an orientation bias affecting the NODDI images. Secondary analyses excluding images with non-uniform gradient schemes generally revealed similar results to primary analyses, where loss of statistical significance in some regions may be due to reduced statistical power within the smaller sample. However, some of the NODDI results should be interpreted with caution as they were altered after excluding the images with non-uniform gradients, suggesting that they could have been influenced by the non-uniform gradients.

Although the participants included in the current study underwent diffusion imaging in the neonatal period, the neonatal data were of insufficient quality for analysis using TBSS and NODDI. However, we have previously described neonatal DTI values for this cohort of children in the corpus callosum [Thompson et al., 2011, 2012], and various other regions-of-interest [Thompson et al., 2014a]. We have also previously described change in DTI values within the corpus callosum between the neonatal period and 7 years of age [Thompson et al., 2015]. In these previous studies of neonatal white matter DTI values, we found that microstructure was altered in VPT children compared with controls in multiple, widespread white matter regions (i.e., the corpus callosum [Thompson et al., 2011] and dorsal prefrontal, orbitofrontal, premotor, subgenual, sensorimotor, mid-temporal, parieto-occipital, inferior occipital, and cerebellar white matter regions [Thompson et al., 2014a]). Together with the current findings, this suggests that altered microstructure is present in widespread white matter regions in VPT children compared with controls in both the neonatal period and 7 years later (in the form of lower FA or higher axon dispersion). Some white matter tracts that appear to display altered microstructure in both the neonatal period and at age 7 years are the corpus callosum, corticospinal tracts, optic radiations, cerebellar tracts, and inferior and superior longitudinal fasciculi. However, it is difficult to compare our previous findings from the neonatal period with the findings from the current study due to the different MRI analysis methods used and different methods for defining white matter regions anatomically.

For our statistical analyses relating perinatal factors to diffusion values at 7 years of age, we chose to focus on three important perinatal factors (GA at birth, birth weight SD score, and neonatal brain abnormality score), given previous studies suggest that these three factors are strong predictors of white matter DTI values in preterm children [Pannek et al., 2014; Thompson et al., 2014a,]. However, we acknowledge that a more detailed analysis of additional perinatal factors in relation to white matter diffusion values in preterm children may be beneficial in future studies.

CONCLUSIONS

This is the first study to apply NODDI to study whole brain white matter microstructure in children born preterm. NODDI revealed that VPT children have higher white matter axon dispersion compared with controls, that neonatal brain abnormalities predict higher axon dispersion in VPT children, and that higher axon dispersion and lower axon density in VPT children are associated with some neurodevelopmental delays. The current study is also one of the first studies to demonstrate associations between NODDI and functional outcomes, although some studies have shown associations between NODDI values in gray matter and functional outcomes in adults [Morris et al., 2016; Nazeri et al., 2015]. White matter tracts that were consistently altered in VPT children included the corpus callosum, internal and external capsules, anterior thalamic radiation and inferior and superior longitudinal fasciculi. Compared with FA alone, NODDI enabled a more detailed and biologically meaningful interpretation of white matter microstructure changes associated with VPT birth, perinatal medical complications and functional outcomes.

ACKNOWLEDGMENTS

We gratefully acknowledge Merilyn Bear for recruitment, Michael Kean and the radiographers at the Royal Children's Hospital, the VIBeS and Developmental Imaging teams at the Murdoch Childrens Research Institute, and the children and families who participated in this study.
The funding sources had no involvement in the study design; in the collection, analysis and interpretation of data; in the writing of the report; and in the decision to submit the article for publication.

REFERENCES

Allin MP, Kontis D, Walshe M, Wyatt J, Barker GJ, Kanaan RA, McGuire P, Rifkin L, Murray RM, Nosarti C (2011): White matter and cognition in adults who were born preterm. PLoS One 6:e24525.

Anderson PJ (2014): Neuropsychological outcomes of children born very preterm. Semin Fetal Neonatal Med 19:90–96.

Andersson JLR, Jenkinson M, Smith S (2007a): Non-Linear Optimisation. Oxford, United Kingdom: FMRIB Centre.

Andersson JLR, Jenkinson M, Smith S (2007b): Non-Linear Registration Aka Spatial Normalisation. Oxford, United Kingdom: FMRIB Centre.

Arpino C, Compagnone E, Montanaro ML, Cacciatore D, De Luca A, Cerulli A, Di Girolamo S, Curatolo P (2010): Preterm birth and neurodevelopmental outcome: A review. Childs Nerv Syst 26:1139–1149.

Bach M, Laun FB, Leemans A, Tax CM, Biessels GJ, Stieltjes B, Maier-Hein KH (2014): Methodological considerations on tract-based spatial statistics (TBSS). NeuroImage 100:358–369.

Billiet T, Madler B, D'Arco F, Peeters R, Deprez S, Plasschaert E, Leemans A, Zhang H, den Bergh BV, Vandenbulcke M, Legius E, Sunaert S, Emsell L (2014): Characterizing the microstructural basis of "unidentified bright objects" in neurofibromatosis type 1: A combined in vivo multicomponent T2 relaxation and multi-shell diffusion MRI analysis. Neuroimage Clin 4: 649–658.

Cole TJ, Freeman JV, Preece MA (1998): British 1990 growth reference centiles for weight, height, body mass index and head circumference fitted by maximum penalized likelihood. Stat Med 17:407–429.

Counsell SJ, Ball G, Edwards AD (2014): New imaging approaches to evaluate newborn brain injury and their role in predicting developmental disorders. Curr Opin Neurol 27:168–175.

de Kieviet JF, Pouwels PJ, Lafeber HN, Vermeulen RJ, van Elburg RM, Oosterlaan J (2014): A crucial role of altered fractional anisotropy in motor problems of very preterm children. Eur J Paediatr Neurol 18:126–133.

Doyle LW (2004): Evaluation of neonatal intensive care for extremely low birth weight infants in Victoria over two decades: I. Effectiveness. Pediatrics 113:505–509.

Duerden EG, Taylor MJ, Miller SP (2013): Brain development in infants born preterm: Looking beyond injury. Semin Pediatr Neurol 20:65–74.

Duvernoy HM (1999): The Human Brain: Surface, Three-Dimensional Sectional Anatomy with MRI, and Blood Supply. Wien/New York: Springer.

Eaton-Rosen Z, Melbourne A, Orasanu E, Cardoso MJ, Modat M, Bainbridge A, Kendall GS, Robertson NJ, Marlow N, Ourselin S (2015): Longitudinal measurement of the developing grey matter in preterm subjects using multi-modal MRI. NeuroImage 111:580–589.

Edden RA, Jones DK (2011): Spatial and orientational heterogeneity in the statistical sensitivity of skeleton-based analyses of diffusion tensor MR imaging data. J Neurosci Methods 201: 213–219.

Eikenes L, Lohaugen GC, Brubakk AM, Skranes J, Haberg AK (2011): Young adults born preterm with very low birth weight demonstrate widespread white matter alterations on brain DTI. NeuroImage 54:1774–1785.

Feldman HM, Lee ES, Loe IM, Yeom KW, Grill-Spector K, Luna B (2012): White matter microstructure on diffusion tensor imaging is associated with conventional magnetic resonance imaging findings and cognitive function in adolescents born preterm. Dev Med Child Neurol 54:809–814.

Goodman R (1997): The Strengths and Difficulties Questionnaire: A research note. J Child Psychol Psychiatry Allied Discipl 38: 581–586.

Groeschel S, Tournier JD, Northam GB, Baldeweg T, Wyatt J, Vollmer B, Connelly A (2014): Identification and interpretation of microstructural abnormalities in motor pathways in adolescents born preterm. NeuroImage 87:209–219.

Henderson SE, Sudgen DA, Barnett AL. 2007. Movement Assessment Battery for Children - Second Edition (Movement ABC-2). London (UK): The Psychological Corporation.

Hua K, Zhang J, Wakana S, Jiang H, Li X, Reich DS, Calabresi PA, Pekar JJ, van Zijl PC, Mori S (2008): Tract probability maps in stereotaxic spaces: Analyses of white matter anatomy and tract-specific quantification. NeuroImage 39:336–347.

Hutchinson EA, De Luca CR, Doyle LW, Roberts G, Anderson PJ (2013): School-age Outcomes of Extremely Preterm or Extremely Low Birth Weight Children. Pediatrics 131:e1053–e1061.

Jenkinson M, Bannister P, Brady M, Smith S (2002): Improved optimization for the robust and accurate linear registration and motion correction of brain images. NeuroImage 17:825–841.

Jespersen SN, Bjarkam CR, Nyengaard JR, Chakravarty MM, Hansen B, Vosegaard T, Ostergaard L, Yablonskiy D, Nielsen NC, Vestergaard-Poulsen P (2010): Neurite density from magnetic resonance diffusion measurements at ultrahigh field: Comparison with light microscopy and electron microscopy. NeuroImage 49:205–216.

Jones DK, Cercignani M (2010): Twenty-five pitfalls in the analysis of diffusion MRI data. NMR Biomed 23:803–820.

Jones DK, Knosche TR, Turner R (2013): White matter integrity, fiber count, and other fallacies: The do's and don'ts of diffusion MRI. NeuroImage 73:239–254.

Kelly CE, Cheong JL, Molloy C, Anderson PJ, Lee KJ, Burnett AC, Connelly A, Doyle LW, Thompson DK (2014): Neural Correlates of Impaired Vision in Adolescents Born Extremely Preterm and/or Extremely Low Birthweight. PLoS One 9: e93188.

Kelly CE, Chan L, Burnett AC, Lee KJ, Connelly A, Anderson PJ, Doyle LW, Cheong JL, Thompson DK (2015a): Brain structural and microstructural alterations associated with cerebral palsy and motor impairments in adolescents born extremely preterm and/or extremely low birthweight. Dev Med Child Neurol

Kelly CE, Cheong JL, Gabra Fam L, Leemans A, Seal ML, Doyle LW, Anderson PJ, Spittle AJ, Thompson DK (2015b): Moderate and late preterm infants exhibit widespread brain white matter microstructure alterations at term-equivalent age relative to term-born controls. Brain Imaging Behav

Kidokoro H, Neil JJ, Inder TE (2013): New MR imaging assessment tool to define brain abnormalities in very preterm infants at term. AJNR Am J Neuroradiol 34:2208–2214.

Kunz N, Zhang H, Vasung L, O'Brien KR, Assaf Y, Lazeyras F, Alexander DC, Huppi PS (2014): Assessing white matter microstructure of the newborn with multi-shell diffusion MRI and biophysical compartment models. NeuroImage 96:288–299.

Lee JD, Park HJ, Park ES, Oh MK, Park B, Rha DW, Cho SR, Kim EY, Park JY, Kim CH, Kim DG, Park CI (2011): Motor pathway injury in patients with periventricular leucomalacia and spastic diplegia. Brain 134:1199–1210.

Leemans A, Jones DK (2009): The B-matrix must be rotated when correcting for subject motion in DTI data. Magn Reson Med 61:1336–1349.

Loe IM, Lee ES, Feldman HM (2013): Attention and internalizing behaviors in relation to white matter in children born preterm. J Dev Behav Pediatr 34:156–164.

Melbourne A, Eaton-Rosen Z, Bainbridge A, Kendall GS, Cardoso MJ, Robertson NJ, Marlow N, Ourselin S (2013): Measurement of myelin in the preterm brain: Multi-compartment diffusion imaging and multi-component T2 relaxometry. Med Image Comput Comput Assist Interv 16:336–344.

Ment LR, Hirtz D, Huppi PS (2009): Imaging biomarkers of outcome in the developing preterm brain. Lancet Neurol 8:1042–1055.

Morris LS, Kundu P, Dowell N, Mechelmans DJ, Favre P, Irvine MA, Robbins TW, Daw N, Bullmore ET, Harrison NA, Voon V (2016): Fronto-striatal organization: Defining functional and microstructural substrates of behavioural flexibility. Cortex 74: 118–133.

Mukherjee P, McKinstry RC (2006): Diffusion tensor imaging and tractography of human brain development. Neuroimaging Clin N Am 16:19–43, vii.

Murray AL, Thompson DK, Pascoe L, Leemans A, Inder TE, Doyle LW, Anderson JF, Anderson PJ (2015): White matter abnormalities and impaired attention abilities in children born very preterm. NeuroImage 124:75–84.

Nazeri A, Chakravarty MM, Rotenberg DJ, Rajji TK, Rathi Y, Michailovich OV, Voineskos AN (2015): Functional consequences of neurite orientation dispersion and density in humans across the adult lifespan. J Neurosci 35:1753–1762.

Nichols TE, Holmes AP (2002): Nonparametric permutation tests for functional neuroimaging: A primer with examples. Hum Brain Mapp 15:1–25.

Owen JP, Chang YS, Pojman NJ, Bukshpun P, Wakahiro ML, Marco EJ, Berman JI, Spiro JE, Chung WK, Buckner RL, Roberts TP, Nagarajan SS, Sherr EH, Mukherjee P (2014): Aberrant white matter microstructure in children with 16p11.2 deletions. J Neurosci 34:6214–6223.

Pandit AS, Ball G, Edwards AD, Counsell SJ (2013): Diffusion magnetic resonance imaging in preterm brain injury. Neuroradiology 55:65–95.

Pannek K, Scheck SM, Colditz PB, Boyd RN, Rose SE (2014): Magnetic resonance diffusion tractography of the preterm infant brain: A systematic review. Dev Med Child Neurol 56:113–124.

Schwarz CG, Reid RI, Gunter JL, Senjem ML, Przybelski SA, Zuk SM, Whitwell JL, Vemuri P, Josephs KA, Kantarci K, Thompson PM, Petersen RC, Jack CR Jr. (2014): Improved DTI registration allows voxel-based analysis that outperforms tract-based spatial statistics. NeuroImage 94:65–78.

Skranes J, Vangberg TR, Kulseng S, Indredavik MS, Evensen KA, Martinussen M, Dale AM, Haraldseth O, Brubakk AM (2007): Clinical findings and white matter abnormalities seen on diffusion tensor imaging in adolescents with very low birth weight. Brain 130:654–666.

Smith SM, Nichols TE (2009): Threshold-free cluster enhancement: Addressing problems of smoothing, threshold dependence and localisation in cluster inference. NeuroImage 44:83–98.

Smith SM, Jenkinson M, Johansen-Berg H, Rueckert D, Nichols TE, Mackay CE, Watkins KE, Ciccarelli O, Cader MZ, Matthews PM, Behrens TE (2006): Tract-based spatial statistics: Voxelwise analysis of multi-subject diffusion data. NeuroImage 31:1487–1505.

Spittle AJ, Orton J (2014): Cerebral palsy and developmental coordination disorder in children born preterm. Semin Fetal Neonatal Med 19:84–89.

Sutton PS, Darmstadt GL (2013): Preterm birth and neurodevelopment: A review of outcomes and recommendations for early identification and cost-effective interventions. J Trop Pediatr 59:258–265.

Thompson DK, Warfield SK, Carlin JB, Pavlovic M, Wang HX, Bear M, Kean MJ, Doyle LW, Egan GF, Inder TE (2007): Perinatal risk factors altering regional brain structure in the preterm infant. Brain 130:667–677.

Thompson DK, Inder TE, Faggian N, Johnston L, Warfield SK, Anderson PJ, Doyle LW, Egan GF (2011): Characterization of the corpus callosum in very preterm and full-term infants utilizing MRI. NeuroImage 55:479–490.

Thompson DK, Inder TE, Faggian N, Warfield SK, Anderson PJ, Doyle LW, Egan GF (2012): Corpus callosum alterations in very preterm infants: Perinatal correlates and 2 year neurodevelopmental outcomes. NeuroImage 59:3571–3581.

Thompson DK, Lee KJ, Egan GF, Warfield SK, Doyle LW, Anderson PJ, Inder TE (2014a): Regional white matter microstructure in very preterm infants: Predictors and 7 year outcomes. Cortex 52:60–74.

Thompson DK, Thai D, Kelly CE, Leemans A, Tournier JD, Kean MJ, Lee KJ, Inder TE, Doyle LW, Anderson PJ, Hunt RW (2014b): Alterations in the optic radiations of very preterm children-Perinatal predictors and relationships with visual outcomes. Neuroimage Clin 4:145–153.

Thompson DK, Lee KJ, van Bijnen L, Leemans A, Pascoe L, Scratch SE, Cheong J, Egan GF, Inder TE, Doyle LW, Anderson PJ (2015): Accelerated corpus callosum development in prematurity predicts improved outcome. Hum Brain Mapp 36:3733–3748.

Timmers I, Zhang H, Bastiani M, Jansma BM, Roebroeck A, Rubio-Gozalbo ME (2015): White matter microstructure pathology in classic galactosemia revealed by neurite orientation dispersion and density imaging. J Inherit Metab Dis 38: 295–304.

Van Hecke W, Leemans A, D'Agostino E, De Backer S, Vandervliet E, Parizel PM, Sijbers J (2007): Nonrigid coregistration of diffusion tensor images using a viscous fluid model and mutual information. IEEE Trans Med Imaging 26:1598–1612.

Van Hecke W, Leemans A, De Backer S, Jeurissen B, Parizel PM, Sijbers J (2010): Comparing isotropic and anisotropic smoothing for voxel-based DTI analyses: A simulation study. Hum Brain Mapp 31:98–114.

Vangberg TR, Skranes J, Dale AM, Martinussen M, Brubakk AM, Haraldseth O (2006): Changes in white matter diffusion anisotropy in adolescents born prematurely. NeuroImage 32:1538–1548.

Veraart J, Sijbers J, Sunaert S, Leemans A, Jeurissen B (2013): Weighted linear least squares estimation of diffusion MRI parameters: Strengths, limitations, and pitfalls. NeuroImage 81:335–346.

Volpe JJ (2009): Brain injury in premature infants: A complex amalgam of destructive and developmental disturbances. Lancet Neurol 8:110–124.

Volpe JJ, Kinney HC, Jensen FE, Rosenberg PA (2011): Reprint of "The developing oligodendrocyte: Key cellular target in brain injury in the premature infant". Int J Dev Neurosci 29:565–582.

Vos SB, Jones DK, Viergever MA, Leemans A (2011): Partial volume effect as a hidden covariate in DTI analyses. NeuroImage 55:1566–1576.

Vos SB, Jones DK, Jeurissen B, Viergever MA, Leemans A (2012): The influence of complex white matter architecture on the mean diffusivity in diffusion tensor MRI of the human brain. NeuroImage 59:2208–2216.

Wechsler D (1999): Wechsler Abbreviated Scale of Intelligence (WASI). New York: The Psychological Corporation.

Wilkinson GS, Robertson GJ (2006): Wide Range Achievement Test- Fourth Edition (WRAT-4). Lutz, FL: Psychological Assessment Resources, Inc.

Winkler AM, Ridgway GR, Webster MA, Smith SM, Nichols TE (2014): Permutation inference for the general linear model. NeuroImage 92:381–397.

Zhang H, Schneider T, Wheeler-Kingshott CA, Alexander DC (2012): NODDI: Practical in vivo neurite orientation dispersion and density imaging of the human brain. NeuroImage 61: 1000–1016.